Domain-wall enhancement of superconductivity in superconductor/ferromagnet hybrids: Case of weak ferromagnets

Flokstra, M.G.; Aarts, J.

Note: To cite this publication please use the final published version (if applicable).

Domain-wall enhancement of superconductivity in superconductor/ferromagnet hybrids: Case of weak ferromagnets

M. Flokstra and J. Aarts

Kamerlingh Onnes Laboratory, Leiden Institute of Physics, P.O. Box 9504, 2300 RA Leiden, The Netherlands

We use magnetotransport measurements to study the influence of the domain structure on the superconducting transition temperature T_c in ferromagnetic (F)/superconducting (S) bilayers and $F/S/F$ trilayers based on Nb and the weak ferromagnet $Cu_{43}Ni_{57}$. By comparing the anisotropic magnetoresistance above T_c with the resistance behavior in the transition and with critical current measurements below T_c, we show that in bilayers enhanced superconductivity is found when the F layer is in a domain state. We also find that, below T_c, the magnetic fields where domains occur are significantly higher than above or around T_c, suggesting that the magnetization rotation in the F layers is influenced by the adjacent superconductor. In trilayers the effects are similar. A domain-state dominated mechanism even for reported spin-valve effects therefore cannot be ruled out.

I. INTRODUCTION

A superconductor (S) and a ferromagnet (F) both show a mean-field order for the electron spins. The exchange field (H_{ex}) in F favors one spin direction, while the superconducting order parameter (Δ) is built up from Cooper pairs consisting of electrons with opposite spins. Bringing these antagonistic types of order into proximity leads to a complex interplay with possible new ground states, and possible consequences for the superconductivity as well as for the magnetism.[1–3] The foremost characteristics of the S/F proximity effect in the case of homogeneous H_{ex} are the oscillatory decay of the induced order parameter in the F metal and the emergence of spin triplet correlations. In special cases this could enable the formation of the spin-equal (long range) triplets, in particular for inhomogeneous exchange fields[4] or half-metallic ferromagnets.[5] The oscillatory order parameter brings about an oscillation of the superconducting transition temperature T_c as a function of the F-layer thickness, which has been observed in various experiments.[6,7] This phenomenon is reasonably well understood and described by theoretical models. As for the existence of long-range triplets, two experiment has been reported thus far,[8,9] but their existence is not yet fully accepted.

Two main consequences of the interplay between magnetism and superconductivity are the $S/F/S$ π junction, and the $F/S/F$ superconducting spin valve. In the π junction the order parameter oscillation in the F metal yields a phase change of π between the superconducting banks, which was demonstrated to exist both by transport experiments[10] and in measurements of the density of states on the F side of and S/F sandwich.[11] The spin-valve exhibits (in theory) re-entrant superconductivity by switching the magnetization of the F banks from parallel (P) to antiparallel (AP), which would lead to a controllable supercurrent through a small field manipulation.[12,13] Theory describing both phenomena is well developed for the case of weak ferromagnetism with homogeneous exchange fields (the quasiclassical Green's functions adequately describe the transport probability of electrons and Cooper pairs). However, inhomogeneities in

H_{ex}, in particular from domains or domain walls, still pose difficulties for both experiment and theory. Also for the case of the spin-valve effect, which it strongest close to T_c where superconductivity is still weakly developed, magnetic domains could also have a significant effect on the superconducting gap and thus on the working of the superconducting spin valve. This is the issue we address below.

By now, various spin-valve systems has been measured. A number of them have Nb as superconductor in combination with weakly magnetic CuNi[14,15] or stronger magnets such as Ni,[16] $Ni_{80}Fe_{20}$ (Permalloy, Py),[17–19] Co, and Fe combined[20] or Co.[21] Moreover, the systems do not only differ in type of magnet, also the method to obtain switching is different. Some use a spin-valve stack with antiferromagnetic $Fe_{50}Mn_{50}$ adjacent to one of the F layers in order to pin its magnetization, while the magnetization of the other layer can rotate freely. This is the case in the reports on Nb/CuNi,[14,15] Nb/Ni,[16] Nb/Py.[18] The other experiments rely on the difference in thickness of the F layers in order to obtain different coercive fields, as in the reports on Nb/Py,[17,19] Nb/(Co,Fe),[20] and Nb/Co.[21] The experiments using a pinning layer confirm the general prediction for the superconducting spin valve: in the P alignment of the two F layers, the transition temperature T_c^P is slightly lower than T_c^{AP} in the AP alignment. The experiments without pinning layer report the reverse behavior, with strong indications that now stray fields and magnetic coupling of the F layers play a role. Taken together, the literature data seem to suggest that the presence of the pinning layer makes a distinction in the outcome of the experiments. This would make sense since domain wall formation in two free layers, as well as the magnetic coupling between the F layers reported for instance in Ref. 19, could be manifestly different in the case that the magnetization of one layer becomes pinned by the antiferromagnet. We are not aware that this observation has been made before, but it makes it possible to understand all the different reports in a unified way.

There is, however, another issue which has not been fully resolved: the size of the apparent spin-valve effects are small compared to theoretical predictions. Changes in T_c are

mostly less than 10 mK, and in bilayer experiments involving Py it was demonstrated that the relative enhancement of superconductivity over domains walls resulted in a similar-sized increase in T_c.[22] For the weak ferromagnets such as $Cu_{1-x}Ni_x$ (with x in the range 0.5–0.6), which played such an important role both in demonstrating π junctions and (apparent) spin switching, it was not yet investigated whether domains in the F layer can enhance superconductivity in a similar way.

Here, we report on a study of $Nb/Cu_{43}Ni_{57}$ bilayers and trilayers where we compare anisotropic magnetoresistance (AMR) effects in the normal state with the magnetoresistance in the superconducting transition and measurements of the depairing (critical) current I_{dp} below T_c, both for micro-structured and large-scale samples. We show that in bilayers enhanced superconductivity is indeed found when the F layer is in a domain state. In the transition this is seen as a decrease in resistance in the field range where domains occur according to AMR. Below the transition it is seen as a maximum in I_{dp} as a function of the in-plane magnetic field. Interestingly, the maximum occurs at significantly higher field values than where the domain state occurs above or in the transition, suggesting that the well-developed superconductivity now influences the mechanism of magnetization rotation in the F layer. Finally, in trilayers we basically make the same observations. A domain state dominated mechanism for spin-valve effects therefore cannot be ruled out.

II. EXPERIMENTAL DETAILS

$Nb/Cu_{43}Ni_{57}$ layers were grown onto Si(100) substrates by DC magnetron sputtering in a ultra-high-vacuum chamber with a background pressure of 10^{-9} mbar and an Ar pressure of 4 μbar with Nb as bottom layer. The $Cu_{43}Ni_{57}$ thickness was kept at 10 nm for all samples, while the Nb layers are 20 nm for the bilayers, and 25 nm for the trilayers. Also, all devices have and addition Nb capping layer (of 1–2 nm thick) on top of the $Cu_{43}Ni_{57}$ top layer. The ratio Cu/Ni in the target is 50/50 (atomic percentage), which results in an approximate 43/57 ratio at the sample. The Curie temperature of the $Cu_{43}Ni_{57}$ is around 150 K, and it has a degree of polarization close to zero (making it a model weak ferromagnet). The purity of the Nb target is 99.95% which yields a T_c of 9.1–9.2 K.

Different samples were used for different bridge widths, although sometimes two bridges were patterned and measured on the same sample. Standard electron beam lithography was used to pattern microsized strips with a length of 40 μm and a width ranging from 1 to 4 μm. These strips were etched with Ar ion-etching (at 2.5 μbar Ar pressure) in a background pressure of 10^{-6} mbar. Au contacts were sputtered in a second deposition step using a lift-off resist-mask technique, with a few monolayers of Ti used as adhesion layer for the Au. The contact geometry is four probe with 10 μm spacing between the voltage probes. Figure 1(a) shows a scanning electron microscope (SEM) image of a 40×2 μm^2 bilayer strip. The contour lines surrounding the high contrast Au leads are Au lift-off residues. Figure 1(c) shows the typical geometry of bond pads and leads. Trilayers
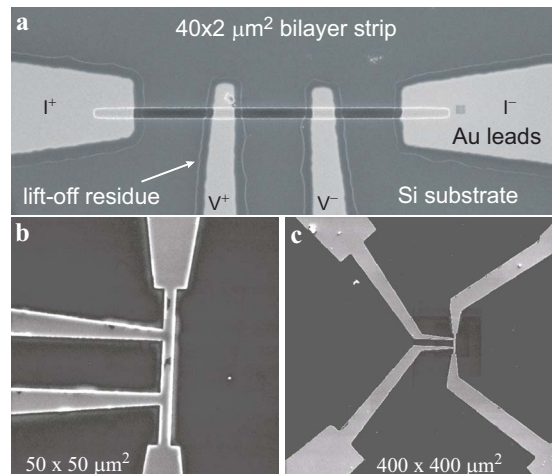

FIG. 1. (Color online) SEM images of a 40×2 μm^2 bilayer devices (a) standard four-probe device, (b) contact included device (marker size 10 μm) and (c) bonding pads and leads (marker size 500 μm). In (a), the bright colored Au leads were deposited using a lift-off mask technique, leaving typical Au residues. The geometry of (c) is used for all devices, the small bright dots near the center are positioning markers.

and macroscopic-sized samples were made using the same recipe, where for the latter the strip dimensions are 2000 $\times 200$ μm^2 with 1000 μm spacing between the voltage probes. The superconducting transition temperature for the bilayer samples, measured after structuring was 6.5 K, except for the 40×1 sample where it was 7.5 K, probably due to a slightly thicker Nb layer. For the trilayers it was 5.9 K (because of the presence of two, instead of one, F layer). The thickness dependence of T_c for plain Nb films and for Nb/F and $F/Nb/F$ were presented in earlier works.[23,24] The two-step process in order to make separate electrical Au contacts to the strips, rather than etch out a full geometry including contacts, is crucial for the experiments, since otherwise the influence of the (magnetic) contact areas can be significant as we show in the Appendix. For those devices with "contacts included" [shown in Fig. 1(b)], strips including leads to the bond pads are all etched out during one step of Ar ion-etching. The micron-sized lateral dimensions brings along two main advantages: it promotes probing states with only few domains, avoiding a large spaghetti of domain states, and the resistance c.q. the cross-section is sufficiently high for AMR measurements and critical current (I_c) measurements. The AMR measurements play a key role in our experiments since they allow to determine if and when domains appear in the ferromagnet just above T_c. This can then be compared to the response of the superconductor to an applied field in and below the transition.

Resistance measurements were done in a standard ^{4}He cryostat with magnetic shielding to provide a low-noise environment, and a superconducting coil to provide the magnetic field (ranging up to 1 T). All field measurements are performed with the externally applied field directed along the strips, which implies the current is parallel to field. For CuNi this should result in a resistance *decrease* when domains are being formed in a initially homogeneous state, similar to the
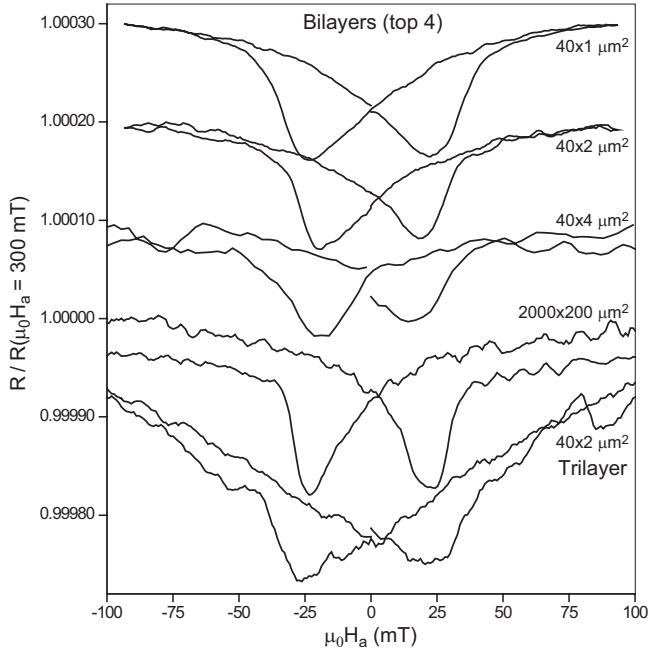
FIG. 2. Resistance normalized to the value at 300 mT as function of an in-plane applied field H_a on Nb/Cu$_{43}$Ni$_{57}$ bilayer strips of 40×1, 40×2, 40×4, and 2000×200 μm^2. Temperatures were in a range between 7.5 and 9 K for the different datasets. The curves are shifted for clarity, each with a value of 1×10^{-4} with respect to the one below. Also shown are data on a 40×2 μm^2 Cu$_{43}$Ni$_{57}$/Nb/Cu$_{43}$Ni$_{57}$ trilayer strip (all with Nb in normal state); these data are not shifted.

behavior of the elemental transition metals Fe, Co, and Ni. At temperatures well below T_c we performed I_c measurements, which probe the gap amplitude in the superconductor. The method for such measurements makes use of pulsed currents, and was described in Ref. 25.

III. RESULTS

Data were obtained for samples with different bridge widths, as well for temperatures above and below T_c, and we present them in the following way. We first give a brief overview of the behavior of the different samples. We then concentrate on the 40×2 μm^2 bilayer strip, which best illustrates most of the physics, before coming back to the samples with different bridge widths. The results of the field-dependent resistance measurements $R(H)$ at a temperature just above T_c are presented in Fig. 2 for bilayer strips with a width of 1 μm, 2 μm, and 4 μm, as well as for the large bilayer structure (2000×200 μm^2), and for a 40×2 μm^2 trilayer strip. The resistance values are normalized to the value measured at 300 mT. The data clearly show hysteresis and resistance dips. The relative resistance change is of order 10^{-4} and the minimum of the dips is close to a field of ± 22 mT. This field we call the dip-field $H_{\mathrm{dip},n}$ (n meaning the normal state) and is generally taken as the coercive field of the ferromagnetic layers. The width of the hysteretic parts is about 50 mT. All bridges show similar values for H_{dip} and the hysteretic width, and they lead to the conclusion that
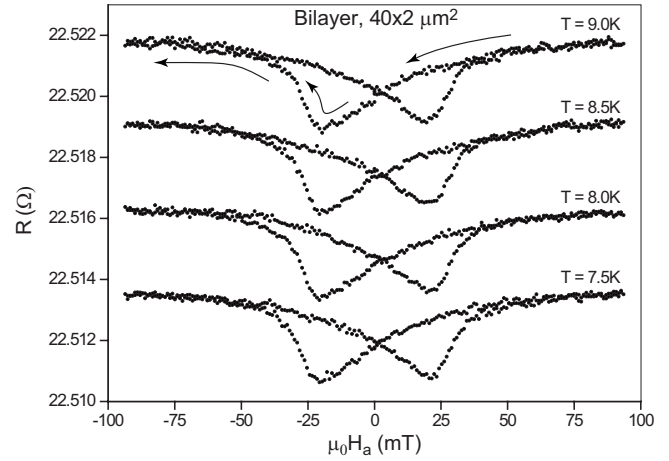

FIG. 3. Resistance R versus in-plane applied field H_a on a 40 $\times 2$ μm^2 Nb/Cu$_{43}$Ni$_{57}$ bilayer strip at several temperatures above the superconducting transition. Arrows in the top curve show the direction of the field sweep starting from high fields.

domains are forming in all our ferromagnetic layers, despite the parallel-field alignment and narrow strips with high-aspect ratio.

A. Results on the 2 μm bridge

Results of $R(H)$ on a 40×2 μm^2 bilayer strip for several temperatures $T > T_c$ are presented in Fig. 3 and illustrate that the values $H_{\mathrm{dip},n}$ are independent of temperature in the range of a few Kelvin above T_c. The same measurements are repeated for $T < T_c$ and shown in Fig. 4, where the resistance is normalized to the value at zero field. The measured signal now comes predominantly from the superconducting layer, which is shorting the ferromagnetic layer by percolation paths. The $R(H)$ are measured at various temperatures along the transition curve shown in Fig. 5, which has an approximate width of 100 mK. The 100 mK width makes that a relative resistance change of 10^{-4} (our typical result in the AMR measurements) corresponds to a temperature change of 0.01 mK. This is below our temperature control accuracy, so we loose track of any AMR features while in the transition area. Again there are two clear dips visible as well as a parabolic-shaped response at higher fields, for all measurement except for the one very near the top of the transition curve at 6.58 K. That one gives a straight line; apparently the superconductor is driven into the normal state by the measurement current, which in all measurements was of the order 2.5×10^8 A/m^2. The relative resistance change $(\delta R)/R$ in the dips is now of order of percents, much larger than the observed AMR effect. Moreover, the size of the dip, meaning the maximum value of the resistance difference δR between forward and backward sweeps, goes through a maximum. Figure 5 shows δR taken from the unnormalized data as function of temperature. It peaks at 6.52 K, which is about halfway in the transition in the steepest part. We can related this to a shift in T_c according to $\delta R = \delta T_c (\partial R/\partial T)$, which comes to a few mK, very similar to the values reported for the CuNi-based (trilayer) spin valve in Ref. 15.
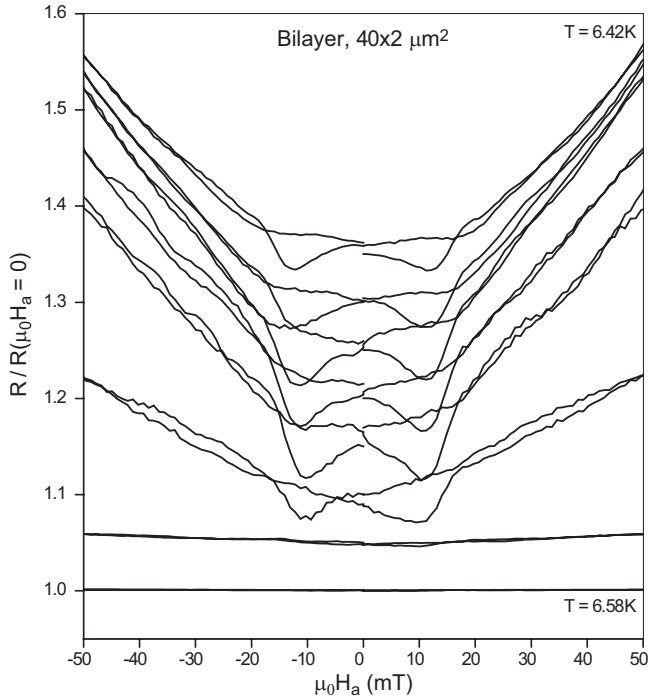
FIG. 4. Resistance normalized to the value at zero field on a 40×2 μm^2 $Nb/Cu_{43}Ni_{57}$ bilayer strip at several temperatures in the transition curve (Nb in superconducting state). The bottom curve is for $T = 6.58$ K. Each subsequent curve is shifted by $+0.05$ with respect to the previous one, with corresponding temperatures 6.55, 6.52, 6.50, 6.48, 6.46, 6.44, and 6.42 K (top curve).

Looking more carefully at the $R(H)$ curve, we notice that (coming from positive fields) the parabolic-shaped curve, which reflects the standard response of the superconductor on a magnetic field, first makes an upward oriented kink around $H = 18$ mT before arriving at the dip, with $H_{dip,s}$ $= -12$ mT (s denoting the superconducting state). The location of the dips and their normalized sizes do not show a
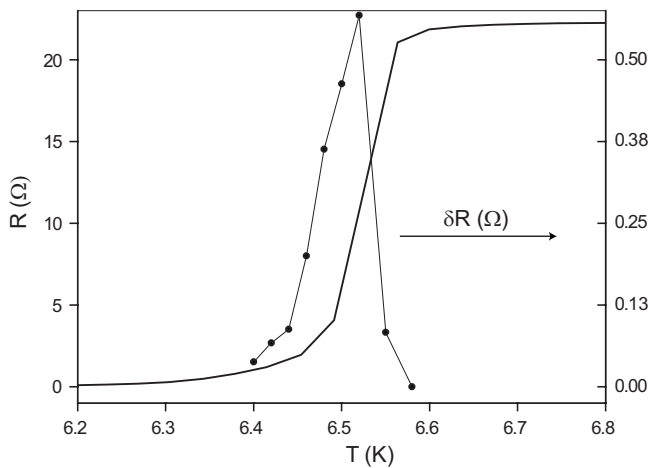

FIG. 5. Temperature variation of the resistance of the 40 $\times 2$ μm^2 $Nb/Cu_{43}Ni_{57}$ bilayer strip in the transition (left-hand scale), which is a typical result for all our devices. Also shown is the temperature variation of the magnitude of the resistance dip δR (right-hand scale).
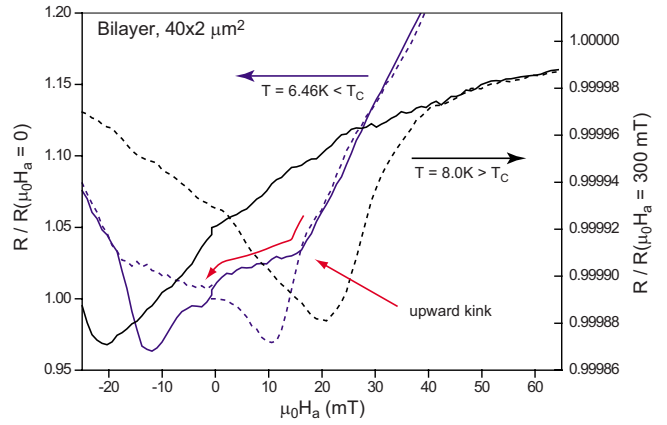

FIG. 6. (Color online) Comparison for T above T_c (right-hand scale) and below T_c (left-hand scale) of the field dependence of the (normalized) resistance R for the 40×2 μm^2 $Nb/Cu_{43}Ni_{57}$ bilayer strip. The solid lines are data taken with *decreasing* field starting from $+300$ mT, as shown by the arrows. The dashed lines are data taken with *increasing* field starting from -300 mT. The upward kink in the decreasing-field data below T_c is also indicated.

strong temperature effect, which is a clear sign that the development of the superconducting gap is not significantly changing the ferromagnetic domain structure. Important to remark, however, is that the dip fields $H_{dip,s}$ are almost a factor two smaller than the dip fields $H_{dip,n}$. We come back to this below, but for the moment we assume that they are still due to the domain state occurring in the $Cu_{43}Ni_{57}$ layer. The dips reflect an enhancement of the (emerging) superconducting state, and therefore indicate that T_c is shifting toward higher values in the domain state, just as seen in previous work on Nb/Py bilayers. In Fig. 6, we compare the $R(H)$ measurements on the 40×2 μm^2 bilayer above and below T_c. It illustrates the difference in dip fields, but also important is to establish that the upward kink seen below T_c in the decreasing field data is still at positive fields in a regime where, according to the AMR, domains are growing. On the other hand, no similar feature is detected in the AMR itself.

We now want to discuss the observations with respect to the change in dip fields and the upward kink. First, note that the amount of screening currents in the superconductor is still negligible, as we work very close to T_c. Second, it is important to realize that the resistance dip occurring in the AMR effect is due to the fact that the resistance in the ferromagnet depends on the angle between the local magnetization M and the current I with, for the case of CuNi, the lowest resistance when $M \perp I$.[26] The resistance minimum found when changing the direction of the magnetization then signifies the maximum amount of domains with a direction perpendicular to the current and the bridge. In the superconducting state, however, the resistance minimum comes about by a different mechanism, since it is determined by the average exchange field sampled by a Cooper pair of characteristic length ξ, which can be quite large close to T_c. There is no reason why the two types of averaging over a domain configuration would yield the same resistance minimum; for instance, a configuration where all of the magnetization is perpendicular to the current would give a strong minimum in
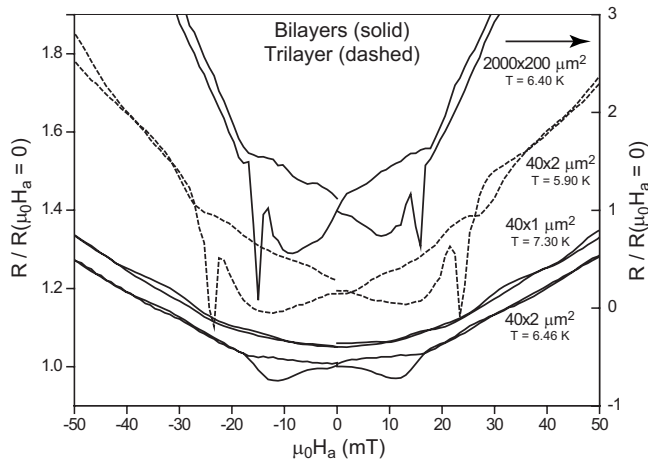
FIG. 7. Normalized resistance measurements on a 40×1, 40×2, and 2000×200 μm^2 Nb/Cu$_{43}$Ni$_{57}$ bilayer (first one shifted by +0.05) and a 40×2 μm^2 Cu$_{43}$Ni$_{57}$/Nb/Cu$_{43}$Ni$_{57}$ trilayer strip (shifted by +0.2). Temperatures are all below the steep part of the corresponding transition curves.

AMR, but no resistance lowering in the superconducting state, since the exchange field in that case is homogeneous. It is interesting to remark that this difference would not be observable in Nb/Py, since in that case the switching was in such a small field range (order 10^{-4} T) that a possible averaging difference would go unnoticed.[22]

That leaves an explanation for the kink feature in $R_s(H)$. Looking again at Fig. 6, it does not seem a coincidence that the quite pronounced kink in the decreasing field data occurs around the coercive field in the increasing field part of the loop. In very similar measurements ($R(H)$ in the resistive transition) on Nb/Py[22] a small increase in R was found at this field point in the hysteresis loop, although it was not visible in the magnetization that domains started to form. Apparently, domain formation and stray field generation starts when the field value comes inside the hysteresis loop even for quite square loops, for which the incipient superconductivity is very sensitive.

B. Other bilayers and trilayers

The 2 μm wide bilayer strips clearly show a decrease in resistance of the superconductor in the domain area of the ferromagnet. The results for other strip widths, specifically for 1 μm and "large" (200 μm wide, 2 mm long) are given in Fig. 7, together with the result on a 40×2 μm^2 trilayer. The curves presented here are all below the steep part of the transition curve. They basically confirm the 2 μm data, but there are some differences. First of all, in the narrower 1 μm strip the resistance dips have completely disappeared, while the AMR data of Fig. 2 definitely indicate the presence of domains. Instead, only the parabolic feature remains. On the other hand, for the larger widths the resistance dips are present at the same field value or a bit lower (large strip) but now, a new sharp dip appears at a field closer to the coercive field. Important of course is that also the new dip signifies lowering of resistance and is therefore not due to stray field enhancement. Without more precise knowledge of the size

and shape of the domains and their evolution, it is difficult to give a solid explanation for these observations. What is known from decoration experiments with magnetic particles is that the typical domain size on large samples is of the order of 0.5 μm.[27] Still, we perceive a hierarchy of events. For the smallest strip AMR detects the occurrence of domains with a component of their magnetization perpendicular to the current, but with a magnetization spread that is not large enough to significantly change the average field that Cooper pairs experience. For the 2 μm strip the domain configuration in the switching is apparently different, and leads to a smaller averaged exchange field. For wider strips the domain state passes through even more configurations. In particular around the coercive field there probably is a large number of small domains, which leads to a sharp resistance dip.

Figure 7 also shows a measurement on the trilayer structured as a 40×2 μm^2 strip. The data show both the shallow dips and the sharp dips, similar to the bilayers with wider bridge widths. The bilayer results exclude that the two dips are due to different switching fields for the two layers, but in the spirit of the hierarchy sketched above, the domain state in the trilayer seems to resemble those of wider bilayers, which suggest a form of coupling between the two layers. From the size of the dip in $R_s(H)$, and the steepness of the transition curves at that temperature, we can estimate the corresponding T_c shift. For all our devices this results in an approximate shift of few mK. We also measured the transition curve at H_{dip} for the cases that the field was set from high positive fields (corresponds to the parabola) and from high-negative fields (corresponds to the dip). In this way we found a shift in T_c of about 1.5 mK, similar to the shift found in the bilayer, and again hardly different from the values reported for the CuNi-based spin valve in Ref. 15.

C. $I_c(H)$ well below T_c

So far we focused on transport measurements around the transition, which consistently show an enhancement of T_c in the domain state of the F layers. To see what happens below T_c we conducted a series of critical current measurements as function of applied field, $I_c(H_a)$ by measuring the current-voltage (I-V) characteristic. We used 3 ms current pulses, with an interval of several seconds and increasing in amplitude until the critical current is reached and the superconductor is driven in the normal state. The sample is initially cooled down in zero-field condition and the first measurement at a fixed temperature always starts in zero applied field. Note that we do not expect vortex formation, since the thickness of the Nb layer (20 nm) is roughly twice the zero-temperature superconducting coherence length, which makes the film two-dimensional for parallel fields. The I-V curves all showed a sharp jump from almost zero voltage to the normal state, as we found before on S films and S/F bilayers.[23,25] An example is given in Fig. 8. The jump indicates that we are measuring a depairing current rather than the onset to vortex flow, which means that the measurement is directly sensitive to the superconducting gap. Also, the value of I_c is well defined due to the sharp transition. The
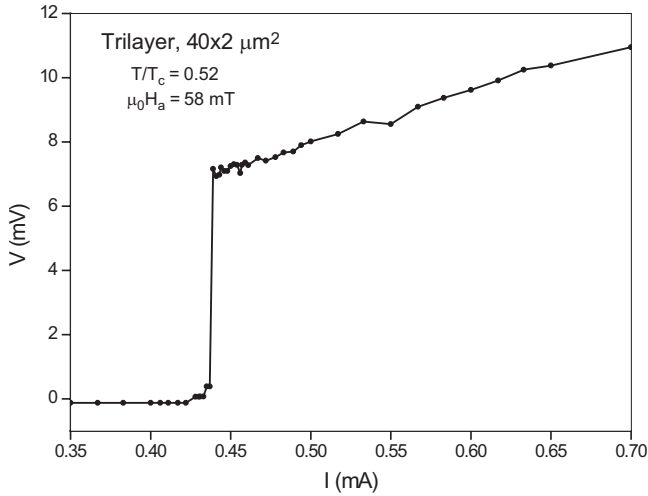
FIG. 8. Voltage V versus current I measured on a 40×2 μm^2 $Cu_{43}Ni_{57}/Nb/Cu_{43}Ni_{57}$ trilayer strip at 4.3 K and 58 mT. The sharp jump at 0.44 mA is taken as a measure for the critical (depairing) current.

results for the 40×2 μm^2 $Cu_{43}Ni_{57}/Nb/Cu_{43}Ni_{57}$ trilayer are shown in Fig. 9, for three temperatures well below T_c, in terms of the reduced temperature $t = T/T_c$ down to $t = 0.5$. All data show the same behavior, with initial constant I_c for increasing H_a, followed by a small maximum of the order of 1%, before a decrease sets in. The field values where the maximum occurs, H_{max}, are in the range 50–60 mT and increase with decreasing temperature. The uncertainty in the determination of I_c is basically the step size for the increase in current (1.8 μA) and therefore significantly below the enhancement of I_c we find around H_{max}. We interpret the enhanced I_c as an enhancement of the superconducting gap, and note that the percentage change is similar to the ob-
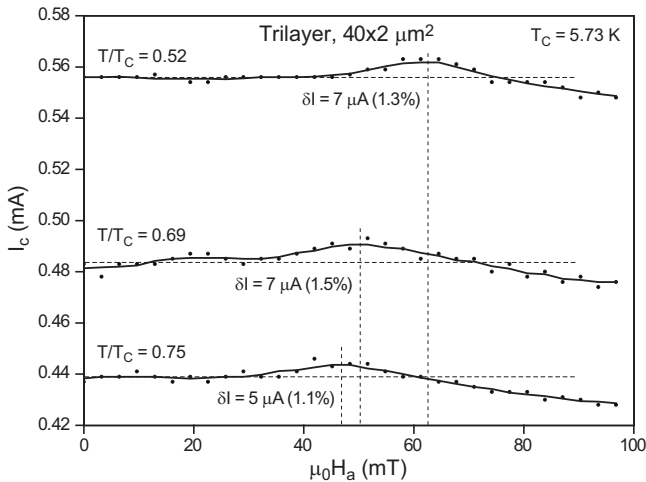

FIG. 9. Critical current measurements I_c as a function of applied magnetic field H_a on a 40×2 μm^2 $Cu_{43}Ni_{57}/Nb/Cu_{43}Ni_{57}$ trilayer strip for different reduced temperature T/T_c as indicated. The value of T_c is 5.73 K. Dotted vertical lines indicated the positions of the maxima in I_c; dotted horizontal lines show the average value of I_c around zero field as reference for the indicated values of increase in I_c at the maximum.
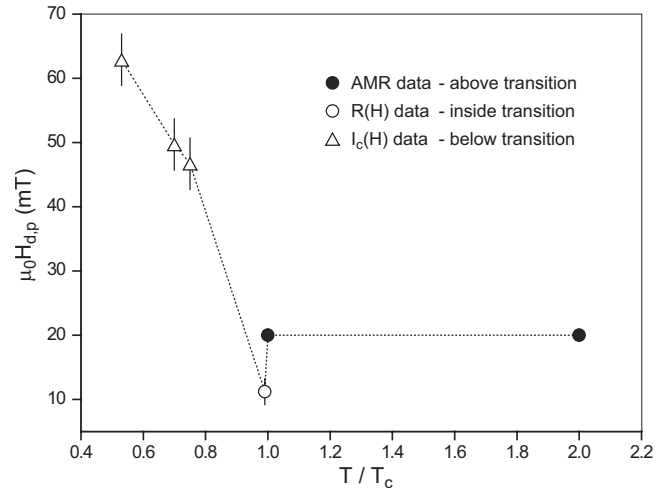

FIG. 10. Collection of the measured dip and peak fields $H_{d,p}$ in our devices as a function of temperature.

served shifts in T_c. The peaks, however, do appears at fields higher than the observed dips fields in our $R(H)$ measurements. In Fig. 10, we combine the values for H_{dip} and H_{max} for the 40×2 μm^2 $Cu_{43}Ni_{57}/Nb/Cu_{43}Ni_{57}$ trilayer. It shows the constant value for H_{dip}^{AMR}, the jump to a lower value in the transition, and then the significant increase well below T_c.

We interpret the maximum in I_c as still caused by the domain state of the F layers. We do not know of similar data in the regime below $T = 0.9$, except for a report on Nb/Co bilayers where an increase in I_c of almost 50% was found at around $t = 0.5$.[28] Such a large value may well be an artefact caused by the sample geometry. As mentioned in Sec. II, the geometry used here consists of simple bars with Au contacts. When the contact pads are included in the etching, all observations can change significantly, and in particular for the I_c enhancement we also find an increase of over 60% as will be shown in the Appendix. The smaller value (of order 1%) also seems intuitively reasonable, since the superconducting order parameter is now well developed and the superconducting coherence length is small, making the sampling of the domain state by the Cooper pair less efficient. That leaves the question of the increase in coercive fields to values above 60 mT. In order to set these in perspective, we can estimate the maximum coercive field $H_{c,m}$ as expected for coherent rotation of the magnetization in the framework of the Stoner-Wohlfart model.[26,29] For the field along the easy axis of magnetization, $H_{c,m}$ equals the anisotropy field $H_{an} = 2K_a/(\mu_0 M_s)$, with K_a the anisotropy constant and M_s the saturation magnetization. Taking a value of 6×10^3 J/m³ for K_a (Ref. 30) and a value of 0.1 T for $\mu_0 M_s$ (Ref. 24) leads to roughly $H_{an} = 0.1$ T, still above the value we find for the coercive fields. This indicates that the superconducting state has a significant effect on the domain structure during the rotation of the magnetization, going in the direction of coherent rotation. As that would mean that the amount of domain walls becomes less, it would be another ground for the small effects observed in the superconductor far below T_c. Incidentally, similar effects of the superconductor on the magnetic state have been reported before. Magnetization measurements using a microfabricated Hall probe on Al/Ni
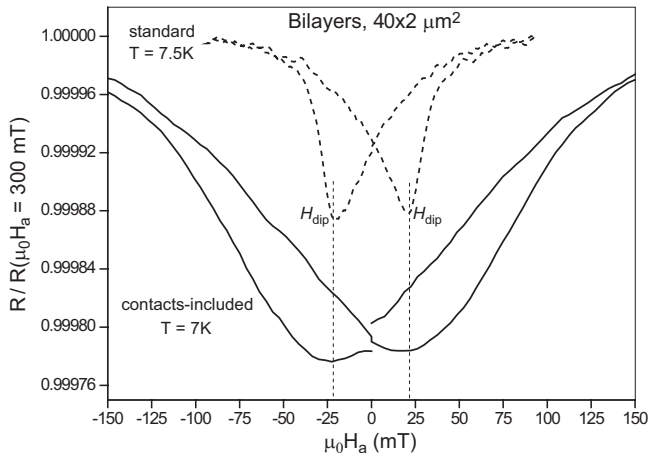
FIG. 11. Resistance measurements on a contact-included 40×2 μm^2 Nb/Cu$_{43}$Ni$_{57}$ bilayer strip, compared to a strip-like standard device of similar size (Nb in the normal state). The temperatures of the measurements (7.5 and 7 K) are just above T_c for both devices. The values of the dip field are indicated with the dotted lines.

submicron samples showed that shielding currents can reshuffle magnetic domains.[31] Similarly, magnetization measurements by SQUID magnetometry on S/F multilayers demonstrated changes in the magnetic state of the F layers in response to the onset of superconductivity.[32,33]

IV. CONCLUSIONS

In conclusion, we investigated the effect of magnetic domains on a superconductor for the case of weakly ferromagnetic Cu$_{43}$Ni$_{57}$ by comparing magnetotransport measurements above and below the superconducting transition, both for bilayers and for trilayers resembling a spin-valve geometry, and for small structures as well as for large samples. We generally find that above the transition the resistance change is dominated by the AMR effect of the ferromagnetic layer (with a relative change of order 10^{-4}), while in the transition it is dominated by changes in the superconducting gap (with a relative change of order 10^{-1}). The AMR measurements show that domains are appearing in all our devices even down to the smallest bridges of 1 μm wide, with nearly identical hysteretic behavior and a coercive field value of 22 mT. In the samples with a 2 μm bridge a small but clear enhancement of T_c is found inside the transition, which we claim to be due to the presence of magnetic domains. This enhancement is present in a limited field range, somewhat smaller than the range over which domains are present in the ferromagnetic layers. Still in the transition, the largest effect on the resistance is at a different field than the largest dip in the AMR. We believe that this reflects the difference in mechanisms giving rise to the two effects; on the one hand magnetization perpendicular to the current, on the other optimal sampling when the superconducting coherence length and the ferromagnetic domain sizes are of similar order. In samples with wider bridges even two dips are found in the transition, which is qualitatively ascribed to the evolution of

domain states which appears to be possible in these wider samples.

By going to lower temperatures and measuring the critical current (as a measure of the strength of the superconducting gap) we see that this enhancement is still present but the field at which it appears is shifting towards significantly higher values. This we attribute to the increasing strength of the superconductor which is forcing the ferromagnet to switch in a more single domain type of manner.

The results on our microstructured bilayers are very similar to the ones on our large-scale bilayer and microstructured trilayers. All different measurement show enhancement of the superconducting gap with a relative size of a few percent. This is very similar to all previous works on spin valves involving weakly ferromagnetic CuNi, where the mechanism was believed to be the parallel vs antiparallel orientation of the exchange fields. In view of our results, domain formation in the individual F layers should be considered at least as an effect of similar importance.

APPENDIX: THE INFLUENCE OF MAGNETIC CONTACTS

In measurements on the effects of stray fields and the spin valve mechanism in $F/S/F$ trilayers different sample geometries are used. In particular for lithographically structured samples it is tempting to include contact pads in the layout, since then only a single etch step is needed to fabricate the full device. Here, we show that such a "contact-included" geometry behaves very differently from a simple strip which has been contacted with Au leads. A scanning electron microscopy (SEM) image of a contact included strip is shown in Figs. 1(b) and 1(c) shows the geometry of the bonding pads and leads to the strip.

Field-dependent resistance measurements on a contact-included 40×2 μm^2 bilayer for $T > T_c$ and $T < T_c$ are shown in Figs. 11 and 12, respectively, where they are compared to the results obtained on our standard bilayer strip. Above T_c the AMR dip shows a large broadening of about a factor 4, while the coercive field value is about the same with a value close to ± 22 mT. Below T_c the results are not very different, except that the location of the dip has shifted to a higher value coinciding with the observed coercive field. From these resistance measurement the "malfunctioning" of the device is not clear, but it does point towards a coercive field dominated working of the device, from which we have shown is not the underlying mechanism in our strips.

In Fig. 13, we show critical current measurements on a contact-included 40×2 μm^2 trilayer and compare them to the results obtained on the standard trilayer strip. The obvious difference is the size of the peak, which now shows an
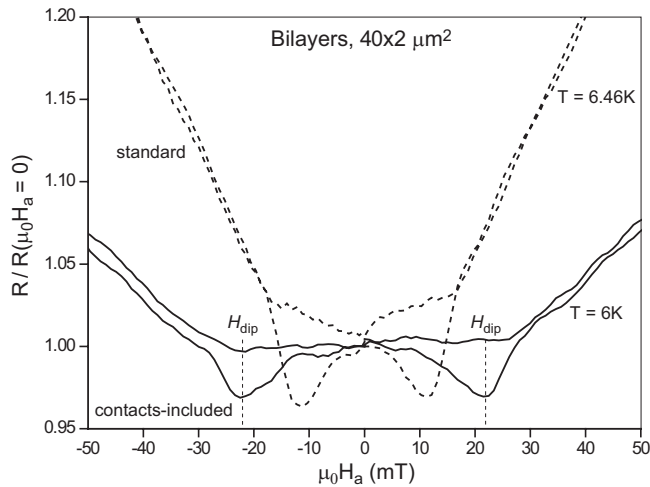
FIG. 12. Resistance measurements on a contact-included 40×2 μm^2 Nb/Cu$_{43}$Ni$_{57}$ bilayer strip, compared to a strip-like standard device of similar size (Nb in the superconducting state). The temperatures of the measurements (6.46 and 6 K) are in the resistive transition for both devices. The values of the dip field are indicated with the dotted lines.

FIG. 13. Critical current measurements I_c as function of applied magnetic field H_a on a contact-included 40×2 μm^2 Cu$_{43}$Ni$_{57}$/Nb/Cu$_{43}$Ni$_{57}$ trilayer strip, for a reduced temperature $T/T_c = 0.69$. The dashed lines show the data from the standard devices displayed in Fig. 9. Also indicated is the critical current increase in the peak as compared to the zero-field value.

increase of nearly 60 percent. The location of the peak compares very well to the ones found on the standard device.

Most likely, the T-shaped contact areas create a bottleneck for the supercurrent. Due to that shape, the magnetic anisotropy energies are likely to dominate the formation process and induce a ve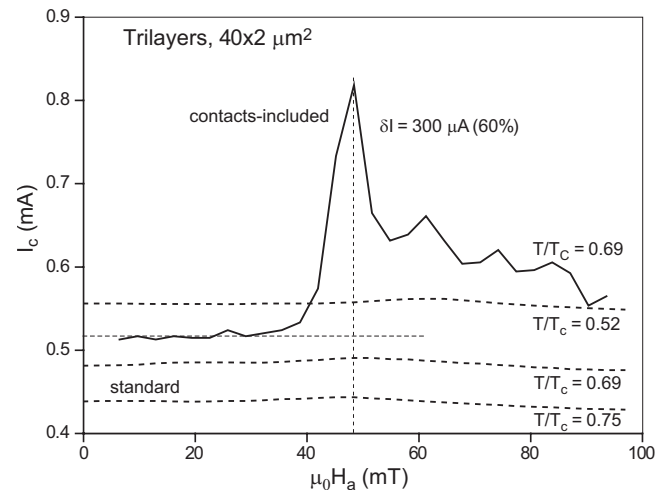ry inhomogeneous magnetic profile localized near the contacts. This explains the large broadening of the AMR curve. Furthermore, this complex domain structure (or rather the stray fields produced by it) strongly suppresses the gap, an effect which apparently disappears at higher fields, resulting in a large increase in critical current.

[1] A. I. Buzdin, Rev. Mod. Phys. **77**, 935 (2005).

[2] I. F. Lyuksyutov and V. L. Pokrovsky, Adv. Phys. **54**, 67 (2005).

[3] F. S. Bergeret, A. F. Volkov, and K. B. Efetov, Rev. Mod. Phys. **77**, 1321 (2005).

[4] F. S. Bergeret, A. F. Volkov, and K. B. Efetov, Phys. Rev. Lett. **86**, 4096 (2001).

[5] M. Eschrig, J. Kopu, J. C. Cuevas, and G. Schön, Phys. Rev. Lett. **90**, 137003 (2003).

[6] Y. Obi, M. Ikebe, T. Kubo, and H. Fujimori, Physica C **317-318**, 149 (1999).

[7] L. Lazar, K. Westerholt, H. Zabel, L. R. Tagirov, Y. V. Goryunov, N. N. Garifyanov, and I. A. Garifullin, Phys. Rev. B **61**, 3711 (2000).

[8] R. S. Keizer, S. T. B. Goennenwein, T. M. Klapwijk, G. Miao, G. Xiao, and A. Gupta, Nature (London) **439**, 825 (2006).

[9] I. Sosnin, H. Cho, V. T. Petrashov, and A. F. Volkov, Phys. Rev. Lett. **96**, 157002 (2006).

[10] V. V. Ryazanov, V. A. Oboznov, A. Y. Rusanov, A. V. Veretennikov, A. A. Golubov, and J. Aarts, Phys. Rev. Lett. **86**, 2427 (2001).

[11] T. Kontos, M. Aprili, J. Lesueur, and X. Grison, Phys. Rev. Lett. **86**, 304 (2001).

[12] L. R. Tagirov, Phys. Rev. Lett. **83**, 2058 (1999).

[13] A. I. Buzdin, A. V. Vedyayev, and N. V. Ryzhanova, Europhys. Lett. **48**, 686 (1999).

[14] J. Y. Gu, C. Y. You, J. S. Jiang, J. Pearson, Y. B. Bazaliy, and S. D. Bader, Phys. Rev. Lett. **89**, 267001 (2002).

[15] A. Potenza and C. H. Marrows, Phys. Rev. B **71**, 180503(R) (2005).

[16] I. C. Moraru, W. P. Pratt, and N. O. Birge, Phys. Rev. Lett. **96**, 037004 (2006).

[17] A. Y. Rusanov, S. Habraken, and J. Aarts, Phys. Rev. B **73**, 060505(R) (2006).

[18] I. C. Moraru, W. P. Pratt, and N. O. Birge, Phys. Rev. B **74**, 220507(R) (2006).

[19] D. Stamopoulos, E. Manios, and M. Pissas, Phys. Rev. B **75**, 184504 (2007).

[20] R. Steiner and P. Ziemann, Phys. Rev. B **74**, 094504 (2006).

[21] G. Carapella, F. Russo, and G. Costabile, Phys. Rev. B **78**, 104529 (2008).

[22] A. Y. Rusanov, M. Hesselberth, J. Aarts, and A. I. Buzdin, Phys. Rev. Lett. **93**, 057002 (2004).

[23] C. Cirillo, A. Rusanov, C. Bell, and J. Aarts, Phys. Rev. B **75**, 174510 (2007).

[24] A. Rusanov, R. Boogaard, M. Hesselberth, H. Sellier, and J. Aarts, Physica C **369**, 300 (2002).

[25] A. Y. Rusanov, M. B. S. Hesselberth, and J. Aarts, Phys. Rev. B **70**, 024510 (2004).

[26] R. O'Handley, *Modern Magnetic Materials* (Wiley and Sons, New York, 2000).

[27] V. V. Ryazanov (private communication).

[28] R. J. Kinsey, G. Burnell, and M. G. Blamire, IEEE Trans. Appl.

Supercond. **11**, 904 (2001).

[29] E. C. Stoner and E. P. Wohlfarth, Philos. Trans. R. Soc. London, Ser. A **240**, 599 (1948).

[30] A. Ruotolo, C. Bell, C. W. Leung, and M. G. Blamire, J. Appl. Phys. **96**, 512 (2004).

[31] S. V. Dubonos, A. K. Geim, K. S. Novoselov, and I. V. Grig-orieva, Phys. Rev. B **65**, 220513(R) (2002).

[32] H.-Y. Wu, J. Ni, J.-W. Cai, Z.-H. Cheng, and Y. Sun, Phys. Rev. B **76**, 024416 (2007).

[33] C. Monton, F. de la Cruz, and J. Guimpel, Phys. Rev. B **77**, 104521 (2008).